A High-Order Kinetic Energy Conserving Scheme for Compressible Large-Eddy Simulation

Francois Cadieux, Michael Barad, and Cetin Kiris

NASA Ames Research Center

Tenth International Conference on
Computational Fluid Dynamics (ICCFD10),
Barcelona, Spain, July 9-13, 2018

- NASA Transformational Tools and Technologies Project (T^3)

- NASA Advanced Supercomputing (NAS) facility

- Colleagues in NASA ARC Computational Aerosciences branch

Motivation

NASA CFD 2030 Vision

The use of CFD in the aerospace design process is severely limited by the inability to accurately and reliably predict turbulent flows with significant regions of separation. [Slotnick et al., 2014].

Key advances that will help solve this problem at non-prohibitive computational cost include:

- Large-eddy simulation (LES) and scale-resolving methods (e.g. hybrid RANS LES)

- Higher order accurate numerical methods

- Minimizing or controlling numerical dissipation

What is numerical dissipation?

We generally want the solution to the compressible Navier-Stokes equations

$$\frac{\partial W_i}{\partial t} = -\frac{\partial F_{\text{conv}}}{\partial x_j} + \frac{\partial F_{visc}}{\partial x_j}$$

but if we use centered interpolation to the faces and centered flux differences, we get numerical instabilities.

So instead, we solve different equations that limit what values the fluxes can take

$$\frac{\partial W_i}{\partial t} = -\frac{\partial}{\partial x_j}(F_{\text{conv}} + F^*) + \frac{\partial F_{visc}}{\partial x_j}$$

to stabilize the scheme, and given fine enough resolution, solution should converge to the original equation because generally $F^* = f(\Delta x^r)$, and $r >= 2$.

Why should anyone care?

- Success of LES methodology hinges on the amount and location of dissipation
  - added by numerics (in the case of implicit LES)
  - by a subgrid-scale (SGS) model (in the case of explicit LES)

  being just enough to account for the unresolved dissipative scales.

- The interplay between dissipation due to numerical scheme, SGS model, and grid resolution is the primary suspect for why researchers report non-monotonic convergence of LES results to DNS or experimental benchmarks

How do we solve this problem?

1. Increase the mesh resolution in key areas,

2. Decrease or remove contribution from SGS model,

3. Modify the numerics so we don't add ANY dissipation away from discontinuities.

What is the benefit of conserving kinetic energy?

- A scheme that conserves mass, momentum, total energy, *and kinetic energy* (when $\mu = 0$) is numerically stable for any smooth flow at any Reynolds number (on periodic grids) [Morinishi, 2010, Brouwer et al., 2014]

- Schemes that consistently use skew-symmetric form for momentum *and energy equation* do not suffer from spurious transfer of energy from kinetic to internal energy even when shocklets are present [Pirozzoli, 2011, Kuya and Kawai, 2018]

- Achieve better results at lower resolution: target dissipation to SGS turbulence and shocks only

Method: Exploiting skew-symmetry

Start from momentum equation in divergence form:

$$\frac{\partial \rho u_i}{\partial t} = \frac{\partial}{\partial x_j}(-\rho u_j u_i - p\delta_{ij} + \tau_{ij})$$

Use product rule on all quadratic or higher terms

$$\frac{1}{2}\left(\frac{\partial \rho u_i}{\partial t} + \rho\frac{\partial u_i}{\partial t} + u_i\frac{\partial \rho}{\partial t}\right) = -\frac{1}{2}\left(\frac{\partial}{\partial x_j}(\rho u_j u_i) + \rho u_j\frac{\partial u_i}{\partial x_j} + u_i\frac{\partial}{\partial x_j}(\rho u_j)\right)$$
$$+ \frac{\partial}{\partial x_j}(-p\delta_{ij} + \tau_{ij})$$

Substitute in $\frac{\partial \rho}{\partial t} = -\frac{\partial}{\partial x_j}(\rho u_j)$ to obtain skew-symmetric form

$$\frac{1}{2}\left(\frac{\partial \rho u_i}{\partial t} + \rho\frac{\partial u_i}{\partial t}\right) = -\frac{1}{2}\left(\frac{\partial}{\partial x_j}(\rho u_j u_i) + \rho u_j\frac{\partial u_i}{\partial x_j}\right) + \frac{\partial}{\partial x_j}(-p\delta_{ij} + \tau_{ij})$$

Method: Integration by parts

Let $\phi\partial u + \partial\phi u = \mathbf{A}u$, where $\mathbf{A}$ is a skew-symmetric operator. Use integration by parts with test functions v, w to show that

$$\int_\Omega v\mathbf{A}w \, \mathrm{d}\Omega = \int_\Omega v(\phi\partial w + \partial\phi w) \, \mathrm{d}\Omega$$

$$= -\int_\Omega w(\phi\partial v + \partial\phi v) \, \mathrm{d}\Omega$$

$$= -\int_\Omega w\mathbf{A}v \, \mathrm{d}\Omega,$$

such that

$$\int_\Omega u\mathbf{A}u \, \mathrm{d}\Omega = 0.$$

In practice, need to use symmetric derivative operators: $\mathbf{D} = -\mathbf{D}^\mathsf{T}$, where $\mathbf{D}u \approx \partial u$ for this property to hold [Brouwer et al., 2014].

Method: Kinetic energy conservation

To obtain the kinetic energy equation we multiply both sides of skew-symmetric momentum equation by u_i

$$LHS = \frac{1}{2}u_i\left(\frac{\partial \rho u_i}{\partial t} + \rho\frac{\partial u_i}{\partial t}\right) = \frac{1}{2}\left(\frac{\partial \rho\frac{1}{2}u_i u_i}{\partial t} + \rho\frac{\partial \frac{1}{2}u_i u_i}{\partial t}\right)$$

and use integration by parts to show that the momentum contribution to RHS goes to zero for periodic BC

$$\int_V -\frac{1}{2}u_i\left(\frac{\partial}{\partial x_j}(\rho u_j u_i) + \rho u_j\frac{\partial u_i}{\partial x_j}\right)\,\mathrm{d}V = 0$$

meaning that kinetic energy is only affected by friction and pressure work terms

$$\frac{\partial}{\partial t}\int_V \frac{1}{2}\rho u_i u_i\,\mathrm{d}V = \int_V u_i\frac{\partial}{\partial x_j}(-p\delta_{ij} + \tau_{ij})\,\mathrm{d}V$$

Method: $\sqrt{\rho}$ scaling

We use the [Morinishi, 2010] trick to simplify the LHS of the momentum equation

$$\frac{1}{2}\left(\frac{\partial \rho u_i}{\partial t} + \rho \frac{\partial u_i}{\partial t}\right) = \left(\frac{\partial \rho u_i}{\partial t} - \frac{u_i}{2}\frac{\partial \rho}{\partial t}\right)$$
$$= \left(\rho \frac{\partial u_i}{\partial t} + \frac{u_i}{2}\frac{\partial \rho}{\partial t}\right)$$
$$= \sqrt{\rho}\frac{\partial \sqrt{\rho} u_i}{\partial t}$$

And the resulting momentum equation then becomes:

$$\sqrt{\rho}\frac{\partial \sqrt{\rho} u_i}{\partial t} = = -\frac{1}{2}\left(\frac{\partial}{\partial x_j}(\rho u_j u_i) + \rho u_j \frac{\partial u_i}{\partial x_j}\right) + \frac{\partial}{\partial x_j}(-p\delta_{ij} + \tau_{ij})$$

Method: Energy equation

We start from the total energy equation, and expand E_k terms:

$$\frac{\partial}{\partial t}(\rho E) = \frac{\partial}{\partial t}(\rho(e + E_k)) = \frac{\partial}{\partial t}(\rho e) + \frac{\partial E_k}{\partial t}$$

$$= -\frac{\partial}{\partial x_j}(\rho u_j(e + E_k) + p u_j - u_i \tau_{ij})$$

$$= -\frac{\partial}{\partial x_j}(\rho u_j e + p u_j - u_i \tau_{ij})$$

$$- \frac{1}{2}\left(\frac{\partial}{\partial x_j}(\rho u_j E_k) + \rho u_j \frac{\partial E_k}{\partial x_j} + E_k \frac{\partial \rho u_j}{\partial x_j}\right)$$

Method: From total to internal energy equation

Then we substitute in equation for $\frac{\partial E_k}{\partial t}$, eliminate terms, and expand internal energy terms for consistency

$$\frac{\partial E_k}{\partial t} = -\frac{1}{2}\left(\frac{\partial}{\partial x_j}(\rho u_j E_k) + \rho u_j \frac{\partial E_k}{\partial x_j} + E_k \frac{\partial \rho u_j}{\partial x_j}\right) + u_i \frac{\partial}{\partial x_j}(-p\delta_{ij} + \tau_{ij})$$

So we obtain a different equation for internal energy than previous authors

$$\frac{\partial}{\partial t}(\rho e) = -\frac{1}{2}\left(\frac{\partial}{\partial x_j}(\rho u_j e) + \rho u_j \frac{\partial e}{\partial x_j} + e\frac{\partial \rho u_j}{\partial x_j}\right)$$
$$-\frac{\partial}{\partial x_j}(p u_j - u_i \tau_{ij}) - \frac{\partial q_j}{\partial x_j}$$
$$+u_i \frac{\partial p}{\partial x_i} - u_i \frac{\partial \tau_{ij}}{\partial x_j}$$

Method: Internal energy equation

We use the product rule to expand and cancel pressure and friction terms and use $\frac{\partial \phi}{\partial t} = 2\sqrt{\phi}\frac{\partial \sqrt{\phi}}{\partial t}$:

$$2\sqrt{\rho e}\frac{\partial \sqrt{\rho e}}{\partial t} = -\frac{1}{2}\left(\frac{\partial}{\partial x_j}(\rho u_j e) + \rho u_j \frac{\partial e}{\partial x_j} + e\frac{\partial \rho u_j}{\partial x_j}\right)$$
$$-\frac{1}{2}\left(\frac{\partial}{\partial x_j}(p u_j) + p\frac{\partial u_j}{\partial x_j} - u_j\frac{\partial p}{\partial x_j}\right) + \tau_{ij}\frac{\partial u_i}{\partial x_j} - \frac{\partial q_j}{\partial x_j}$$

But terms leftover from the kinetic energy equation are volumetric terms, not fluxes:

$$u_j\frac{\partial p}{\partial x_j}, \quad p\frac{\partial u_j}{\partial x_j}, \quad \tau_{ij}\frac{\partial u_i}{\partial x_j}$$

So we cannot use the Pirozzoli trick [Pirozzoli, 2011] and efficiently use fluxes at the half-points/faces...

Method: Conservative finite differences

So instead we take the high-order conservative finite difference approach and solve this set of equations where each derivative operator $\frac{\partial}{\partial x_j}$ is a 6$^{\text{th}}$ order centered difference stencil $\mathbf{D} = -\mathbf{D}^{\mathsf{T}}$:

$$\frac{\partial \sqrt{\rho}}{\partial t} = -\frac{1}{2\sqrt{\rho}}\frac{\partial}{\partial x_j}(\rho u_j),$$

$$\frac{\partial \sqrt{\rho} u_i}{\partial t} = \frac{1}{\sqrt{\rho}}\left[-\frac{1}{2}\left(\frac{\partial}{\partial x_j}(\rho u_j u_i) + \rho u_j \frac{\partial u_i}{\partial x_j} \right) - \frac{\partial p}{\partial x_i} + \frac{\partial \tau_{ij}}{\partial x_j} \right]$$

$$\frac{\partial \sqrt{\rho e}}{\partial t} = \frac{1}{2\sqrt{\rho e}}\left[-\frac{1}{2}\left(\frac{\partial}{\partial x_j}(\rho e u_j) + \rho u_j \frac{\partial e}{\partial x_j} + e\frac{\partial \rho u_j}{\partial x_j} \right) \right.$$

$$\left. -\frac{1}{2}\left(\frac{\partial}{\partial x_j}(p u_j) + p\frac{\partial u_j}{\partial x_j} - u_j \frac{\partial p}{\partial x_j} \right) + \tau_{ij}\frac{\partial u_i}{\partial x_j} - \frac{\partial q_j}{\partial x_j} \right]$$

Method: Implementation details

Cartesian immersed boundary treatment

- Deal with immersed boundary with simple ghost cell method (GCM) [Mittal et al., 2008] and ghost-in-fluid (GIF) [Nakahashi, 2011] method for thin geometry
- Drop order close to body to ensure central difference stencil doesn't go beyond valid ghost cell data

Boundary conditions and adaptive mesh refinement (AMR)

- Use a sponge layer *or* add explicit 5th order artificial dissipation (AD) [Pulliam, 2011] surgically near non-periodic boundary points with $\epsilon_5 = 0.01$
- Use higher order interpolation *or* surgical addition of AD near 2:1 fine-to-coarse interfaces [Pantano et al., 2007]
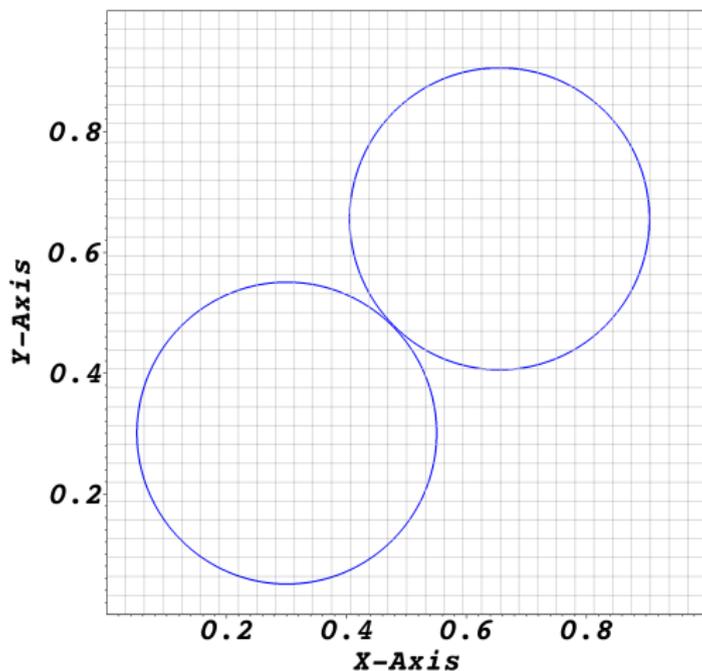
Cut of the two spheres in the domain used for MMS tests with geometry and the starting mesh (before any refinement).

Results: MMS convergence with geometry

L_∞ norm of the discretization error obtained from inviscid MMS with two spheres close together. Convergence rates are shown in parenthesis.

Mesh	Mass		Momentum		Total Energy	
	WENO6	KECons	WENO6	KECons	WENO6	KECons
m0	1.9E-02	7.0E-05	4.4E-01	4.0E-02	1.3E+03	6.2E+00
m1	1.0E-02 (0.89)	1.8E-05 (2.01)	2.1E-01 (1.03)	1.0E-02 (2.00)	6.7E+02 (0.97)	1.5E+00 (2.01)
m2	5.0E-03 (1.00)	4.4E-06 (2.01)	1.1E-01 (1.02)	2.5E-03 (1.99)	3.4E+02 (0.98)	3.8E-01 (2.00)

L_∞ norm of the discretization error obtained from MMS for the Navier-Stokes equations with $\mu = 10^{10}$ and with two spheres close together.

Mesh	Mass		Momentum		Total Energy	
	WENO6	KECons	WENO6	KECons	WENO6	KECons
m0	1.9E-02	7.0E-05	1.2E+08	1.3E+08	7.7E+12	3.6E+12
m1	1.0E-02 (0.89)	1.8E-05 (2.01)	3.1E+07 (1.99)	3.2E+07 (1.97)	2.0E+12 (1.99)	8.6E+11 (2.07)
m2	5.0E-03 (1.01)	4.4E-06 (2.01)	7.9E+06 (1.99)	8.1E+06 (1.99)	4.9E+11 (2.00)	2.1E+11 (2.02)
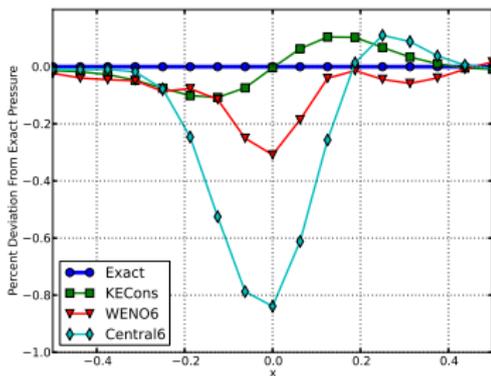
$(p_{\text{exact}} - p)/p_{\text{exact}} \times 100\%$
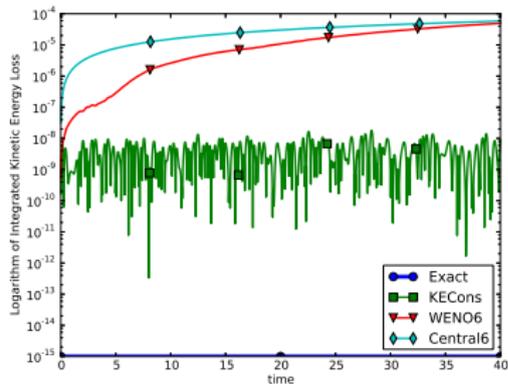
$\log(\int_\Omega K_{\text{exact}} dV - \int_\Omega K dV)$, where $K = \frac{1}{2}\rho u_i u_i$

Inviscid isentropic vortex propagation in Mach 0.5 flow (max Mach = 0.75) in periodic domain discretized with 32^2 evenly-spaced cells, integrated in time for 10 flow-throughs with $\Delta t = 0.01$ (CFL=0.28 at start) with explicit RK4.

Results: Inviscid Taylor-Green Vortex
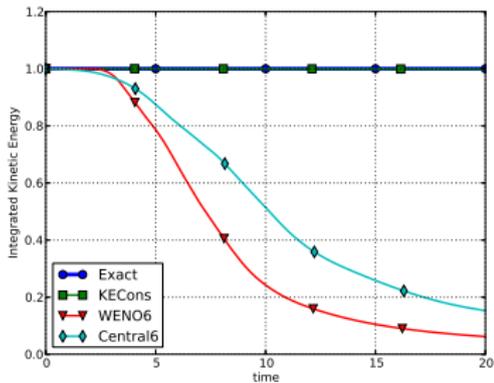
Non-dimensional integrated kinetic energy
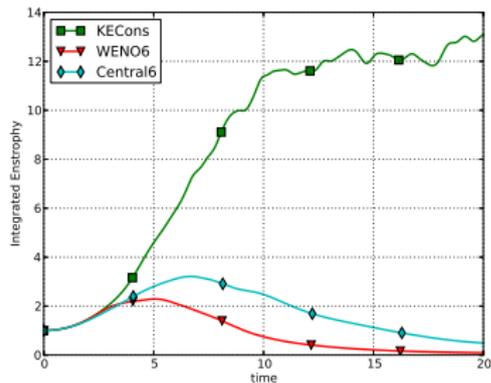
Integrated enstrophy

Inviscid Taylor-Green vortex at Mach 0.1, performed with 32^3 resolution and integrated in time using RK4 for 20 flow-throughs with $\Delta t = 0.0014$, which gives a CFL number near 0.5.
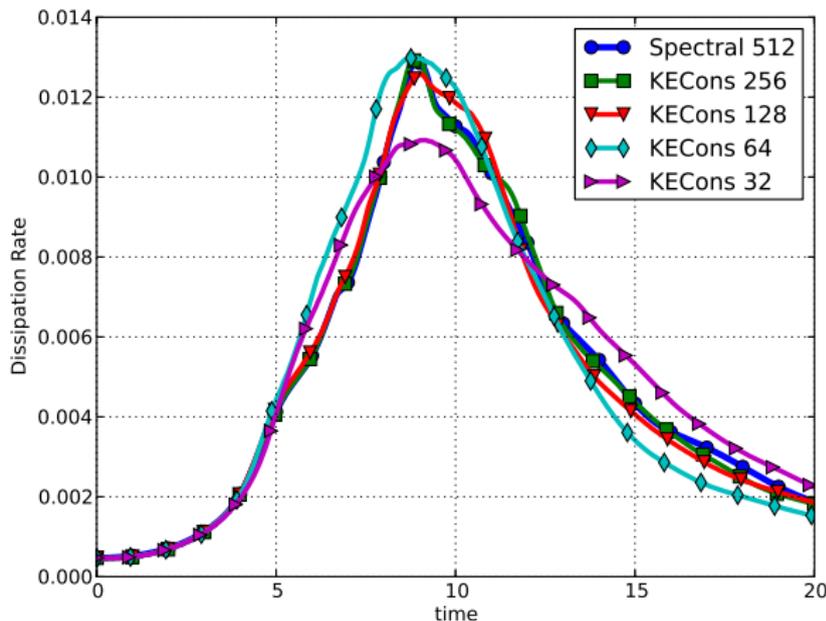
Taylor-Green Vortex results for kinetic energy conserving scheme (KECONS) with the dynamic σ SGS model at different grid resolutions, integrated in time with RK4 and fixed CFL=0.5
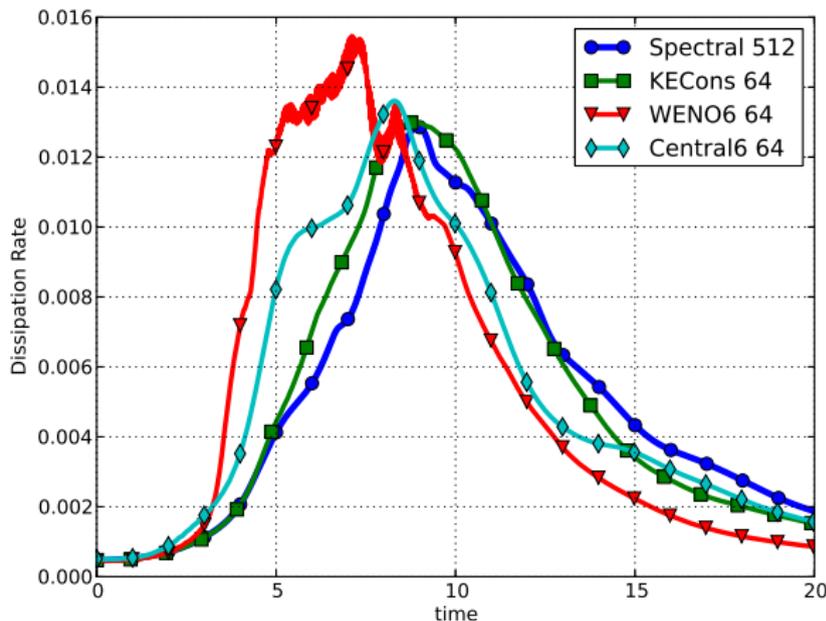
Taylor-Green Vortex results for kinetic energy conserving scheme (KECONS) with the dynamic σ SGS model compared to ILES with different finite difference schemes at 64^3 resolution, integrated in time with RK4 and fixed CFL=0.5
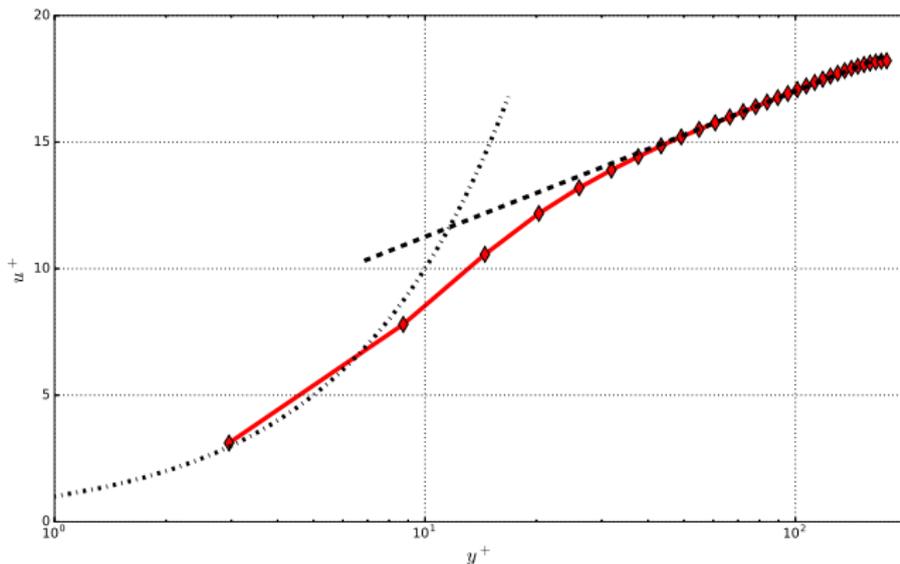
Mean velocity profile: KECons run at Mach= 0.2 with σ model at 64^3 resolution $\Delta x^+, \Delta y^+, \Delta z^+ = 17, 5.8, 8.7$ and RK4 with CFL=0.5 (diamonds), law of the wall $u^+ = 2.5\ln(y^+) + 5.5$ (dashes), $u^+ = y^+$ (dash-dots).
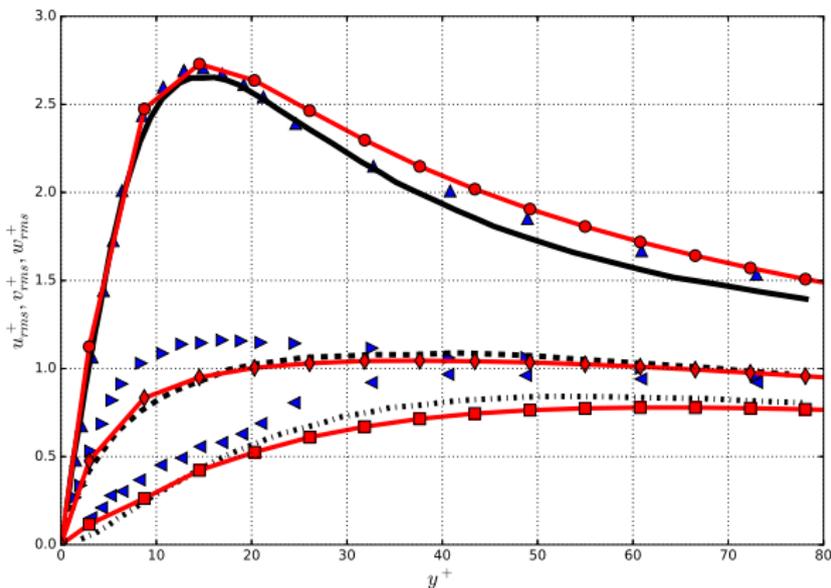
Kreplin & Eckelmann (1979) corrected experimental data
[Kim et al., 1987]: u_{rms}^+ (triangles), v_{rms}^+ (right triangles), w_{rms}^+ (left triangles); DNS [Kim et al., 1987]: u_{rms}^+ (line), v_{rms}^+ (dashes), w_{rms}^+ (dash-dots); KECons 64^3: u_{rms}^+ (circles), v_{rms}^+ (diamonds), w_{rms}^+ (squares).

Time-averaged velocity profiles for flow past a cylinder at $Re_D = 3900$. Experimental PIV Measurements [Parnaudeau et al., 2008] (squares), DNS at $Re = 3300$ [Wissink and Rodi, 2008] (circles), LES [Parnaudeau et al., 2008] (triangles), LES [Kravchenko and Moin, 2000] (diamonds), LAVA WENO6 (dashes), LAVA KECons $+ \sigma$ model (line).

Lessons Learned

- Cross-derivatives are tricky when close to potentially under-resolved immersed boundary geometry

- Implicit Runge-Kutta with Gauss quadrature is not worthwhile: too expensive and too sensitive to sub-iteration convergence (see paper and [Jameson, 2017])

- Moving away from flux at faces requires complete re-write of codebase and different thinking in terms of performance optimization

- Stability of consistent skew-symmetric form is impressive, but perhaps it can be obtained without eschewing flux-form using [Pirozzoli, 2011] trick
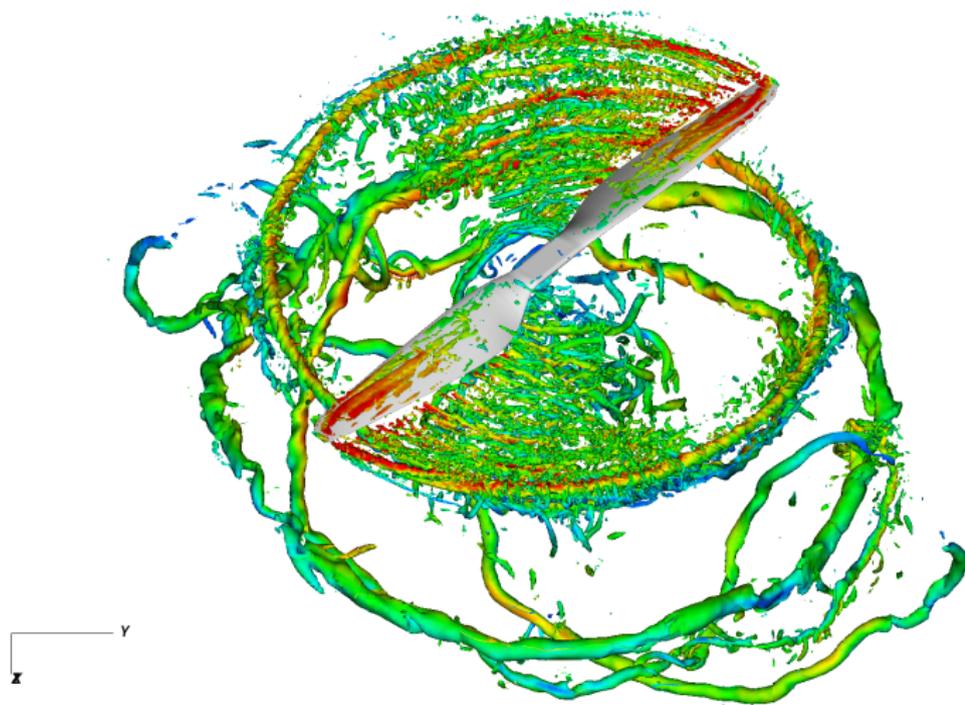
Backup Slides

Method: High order viscous terms

In order to have consistent 6th order derivatives for all terms without requiring more ghost cells, we use the product rule to expand the viscous and diffusion terms

$$
\begin{aligned}
\frac{\partial \tau_{ij}}{\partial x_j} =& \frac{\partial}{\partial x_j}\left(\mu(\frac{\partial u_i}{\partial x_j} + \frac{\partial u_j}{\partial x_i}) + \beta\frac{\partial u_k}{\partial x_k}\delta_{ij}\right) \\
=& \frac{\partial \mu}{\partial x_j}\left(\frac{\partial u_i}{\partial x_j} + \frac{\partial u_j}{\partial x_i}\right) + \frac{\partial \beta}{\partial x_j}\frac{\partial u_k}{\partial x_k}\delta_{i,j} \\
& + \left(\mu(1 + \delta_{i,j}) + \beta\delta_{i,j}\right)\frac{\partial^2 u_i}{\partial x_j^2} + (\mu + \beta)(1 - \delta_{i,j})\frac{\partial^2 u_j}{\partial x_i x_j},
\end{aligned}
$$

$$
\begin{aligned}
\frac{\partial q_j}{\partial x_j} =& \frac{\partial}{\partial x_j}\left(-\kappa\frac{\partial T}{\partial x_j}\right) \\
=& -\frac{\partial \kappa}{\partial x_j}\frac{\partial T}{\partial x_j} - \kappa\frac{\partial^2 T}{\partial x_j^2}
\end{aligned}
$$

Method of manufactured solutions (MMS)

L_∞ norm of the discretization error obtained from inviscid MMS without geometry. Convergence rates are shown in parenthesis.

Mesh	Mass		Momentum		Total Energy	
	WENO6	KECons	WENO6	KECons	WENO6	KECons
m0	3.6E-08	3.3E-08	2.6E-06	2.6E-06	8.4E-04	1.3E-03
m1	5.2E-10 (6.11)	5.3E-10 (5.96)	4.2E-08 (5.98)	4.1E-08 (5.99)	6.1E-06 (7.11)	2.1E-05 (5.97)
m2	8.2E-12 (5.98)	8.3E-12 (5.99)	6.7E-10 (5.98)	6.5E-10 (5.99)	9.9E-08 (5.94)	3.3E-07 (5.99)

L_∞ norm of the discretization error obtained from MMS for the Navier-Stokes equations with $\mu = 10^{10}$. Convergence rates are shown in parenthesis.

Mesh	Mass		Momentum		Total Energy	
	WENO6	KECons	WENO6	KECons	WENO6	KECons
m0	3.7E-08	3.3E-08	1.3E+08	3.0E+04	7.8E+12	1.2E+09
m1	5.3E-10 (6.12)	5.3E-10 (5.96)	3.2E+07 (1.99)	4.7E+02 (5.98)	2.0E+12 (1.99)	1.9E+07 (5.98)
m2	8.3E-12 (5.98)	8.3E-12 (5.99)	7.9E+06 (2.00)	7.6E+00 (5.96)	4.9E+11 (2.00)	3.1E+05 (5.95)

Method: Kinetic energy conservation in time

Need a time integrator that preserves the integration by parts property:

$$\int_t v(\phi \partial_t w + \partial_t \phi w)\,\mathrm{d}t = -\int_t w(\phi \partial_t v + \partial_t \phi v)\,\mathrm{d}t$$

$$\int_t u(\phi \partial_t u + \partial_t \phi u)\,\mathrm{d}t = 0$$

Which restricts us to fully implicit Runge-Kutta schemes:

$$y^{n+1} = y^n + \Delta t \sum_{i=1}^{s} b_i k_i$$

$$k_i = f(Y_i)$$

$$Y_i = y^n + \Delta t \sum_{j=1}^{s} a_{ij} k_j$$

That satisfy $b_i a_{ij} + b_j a_{ji} = b_i b_j$, e.g. Gauss quadratures [Brouwer et al., 2014]
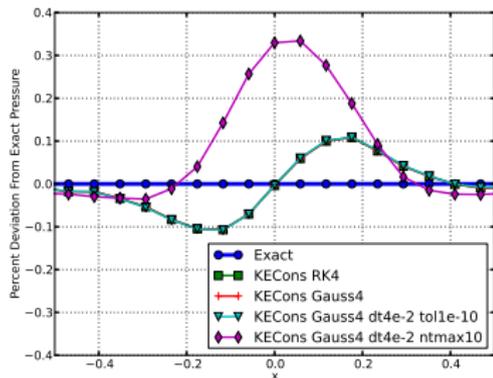
$(p_{\text{exact}} - p)/p_{\text{exact}} \times 100\%$
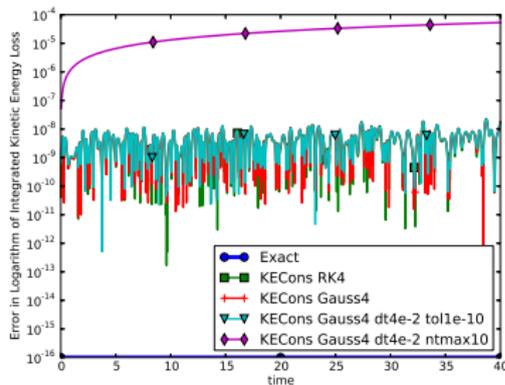
$\log(\int_\Omega K_{\text{exact}} dV - \int_\Omega K dV)$, where $K = \frac{1}{2}\rho u_i u_i$

Comparison of inviscid isentropic vortex propagation results for KECons with explicit RK4 (squares), Gauss4 (crosses), Gauss4 using a 4 times larger time step (triangles), and Gauss4 using a 4 times larger time step and a limit of 10 sub-iterations (diamonds).
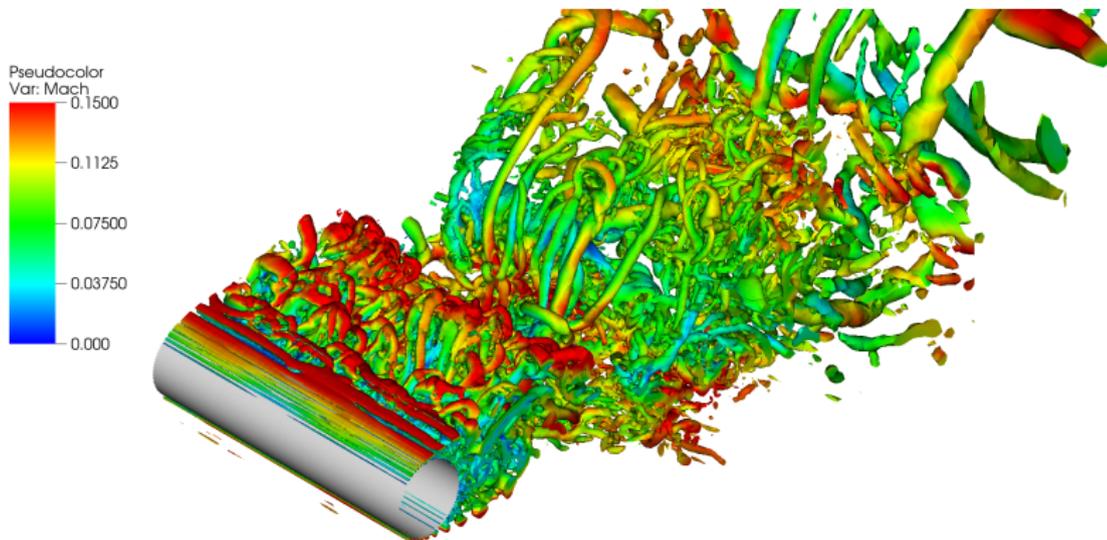
Instantaneous snapshot of iso-surfaces of Q-criterion colored by Mach number for flow past cylinder at $Re_D = 3900$.

Future Work

- Implement shock capturing that will not break conservation properties (e.g. local artificial diffusion (LAD), conservative filtering)

- Implement and validate a wall-model for turbulent boundary layer flows

- Research and implement an energy-stable higher-order interior-only immersed boundary method

Brouwer, J., Reiss, J., and Sesterhenn, J. (2014).
Conservative time integrators of arbitrary order for skew-symmetric finite-difference discretizations of compressible flow.
Computers & Fluids, 100:1 – 12.

Jameson, A. (2017).
Evaluation of fully implicit runge kutta schemes for unsteady flow calculations.
Journal of Scientific Computing, 73(2-3):819–852.

Kim, J., Moin, P., and Moser, R. (1987).
Turbulence statistics in fully developed channel flow at low reynolds number.
Journal of fluid mechanics, 177:133–166.

Kravchenko, A. G. and Moin, P. (2000).
Numerical studies of flow over a circular cylinder at re d= 3900.
Physics of fluids, 12(2):403–417.

Kuya, Y. and Kawai, S. (2018).
Physically consistent formulations for kinetic energy preservation by quasi-skew-symmetric forms.
In *2018 AIAA Aerospace Sciences Meeting*, page 1563.

Mittal, R., Dong, H., Bozkurttas, M., Najjar, F., Vargas, A., and von Loebbecke, A. (2008).
A versatile sharp interface immersed boundary method for incompressible flows with complex boundaries.
Journal of computational physics, 227(10):4825–4852.

Morinishi, Y. (2010).
Skew-symmetric form of convective terms and fully conservative finite difference schemes for variable density low-mach number flows.
Journal of Computational Physics, 229(2):276–300.

Nakahashi, K. (2011).
Immersed boundary method for compressible euler equations in the building-cube method.
In *20th AIAA Computational Fluid Dynamics Conference*, page 3386.

Pantano, C., Deiterding, R., Hill, D. J., and Pullin, D. I. (2007).
A low numerical dissipation patch-based adaptive mesh refinement method for large-eddy simulation of compressible flows.
Journal of Computational Physics, 221(1):63–87.

Parnaudeau, P., Carlier, J., Heitz, D., and Lamballais, E. (2008).
Experimental and numerical studies of the flow over a circular cylinder at reynolds number 3900.
Physics of Fluids, 20(8):085101.

Pirozzoli, S. (2011).
Numerical methods for high-speed flows.
Annual Review of Fluid Mechanics, 43(1):163–194.

Pulliam, T. (2011).
High order accurate finite-difference methods: as seen in overflow.
In *20th AIAA Computational Fluid Dynamics Conference*, page 3851.

Slotnick, J., Khodadoust, A., Alonso, J., Darmofal, D., Gropp, W., Lurie, E., and Mavriplis, D. (2014).
CFD vision 2030 study: a path to revolutionary computational aerosciences.
NASA Technical Report.

Wissink, J. and Rodi, W. (2008).
Numerical study of the near wake of a circular cylinder.
International journal of heat and fluid flow, 29(4):1060–1070.